

AN OPTICAL COUNTERPART CANDIDATE FOR THE ISOLATED NEUTRON STAR RBS1774

S. ZANE¹, R. P. MIGNANI¹, R. TUROLLA^{2,1}, A. TREVES³, F. HABERL⁴, C. MOTCH⁵, L. ZAMPIERI⁶, M. CROPPER¹
Send offprint requests to: sz@mssl.ucl.ac.uk

ABSTRACT

Multiwavelength studies of the seven identified X-ray dim isolated neutron stars (XDINSs) offer a unique opportunity to investigate their surface thermal and magnetic structure and the matter-radiation interaction in presence of strong gravitational and magnetic fields. As a part of an ongoing campaign aimed at a complete identification and spectral characterization of XDINSs in the optical band, we performed deep imaging with the ESO *Very Large Telescope* (VLT) of the field of the XDINS RBS1774 (1RXS J214303.7 +065419). The recently upgraded *FORS1* instrument mounted on the VLT provided the very first detection of a candidate optical counterpart in the B band. The identification is based on a very good positional coincidence with the X-ray source (chance probability $\sim 2 \times 10^{-3}$). The source has $B=27.4 \pm 0.2$ (1σ confidence level), and the optical flux exceeds the extrapolation of the X-ray blackbody at optical wavelengths by a factor ~ 35 (± 20 at 3σ confidence level). This is barely compatible with thermal emission from the neutron star surface, unless the source distance is $d \approx 200\text{--}300$ pc, and the star is an almost aligned rotator or its spin axis is nearly aligned with the line of sight. At the same time, such a large optical excess appears difficult to reconcile with rotation-powered magnetospheric emission, unless the source has an extremely large optical emission efficiency. The implications and possible similarities with the optical spectra of other isolated NSs are discussed.

Subject headings: star: individual (RBS1774) — stars: neutron — X-rays: stars — ultraviolet: stars

1. INTRODUCTION

One of the most intriguing results of the ROSAT All Sky Survey has been the detection of seven close-by neutron stars (NSs), with particular characteristics (XDINSs in the following, see Haberl 2007; Van Kerkwijk & Kaplan 2007, for recent reviews). These sources stand apart with respect to other known classes of isolated NSs detected at X-ray energies. Their X-ray spectrum is close to a blackbody, and no evidence of radio emission has been reported so far despite deep searches (e.g. Kondratiev et al. 2008).⁷ They are likely to be endowed with relatively strong magnetic fields, $B \approx 10^{13}\text{--}10^{14}$ G, as inferred from X-ray timing measurements and observations of broad spectral lines (equivalent width $\approx 10\text{--}100$ eV, likely due to proton cyclotron and/or bound-free, bound-bound transitions in H, H-like and He-like atoms). This points toward a possible evolutionary link between XDINSs, “magnetars” (Anomalous X-ray Pulsars and Soft Gamma-Repeaters; see Mereghetti 2008, for a review), and some of the recently discovered rotating radio transients (RRATs; McLaughlin et al. 2006, 2007, see also Heyl & Kulkarni 1998 and Popov, Turolla & Possenti 2006 for a discussion).

Detailed multiwavelength studies of XDINSs are fundamental for tracking their evolutionary history, and for shedding light on their thermal and magnetic surface properties. While the XDINSs have similar spectral properties in the X-rays, in the optical the paucity of multi-band observations prevents a clear spectral characterization. For the XDINSs with a certified counterpart (see e.g. Kaplan 2008, for a recent review) the optical emission lies typically a factor ~ 10 , or more, above the extrapolation of the X-ray blackbody into the optical/UV band. However, while the optical flux closely follows a Rayleigh-Jeans distribution in RX J1856.5-3754, possible deviations from a λ^{-4} behaviour have been reported for RX J0720.4-3125 and RX J1605.3+3249 (Kaplan et al. 2003a; Motch et al. 2003, 2005; Zane et al. 2006). Thus, whether the optical emission from XDINSs is produced by regions of the star surface at a lower temperature (e.g. Pons et al. 2002) or by other mechanisms, such as non-thermal emission from particles in the star magnetosphere or reprocessing of the surface radiation by an optically thin (to X-rays) hydrogen layer surrounding the star (Motch et al. 2003; Zane et al. 2004; Ho et al. 2007), is still under debate.

One of the XDINSs which so far eluded optical identification is RBS1774 (1RXS J214303.7 +065419). This source was firstly identified in a pointed ROSAT/PSPC observation by Zampieri et al. (2001); accurate spectral and timing information were then obtained with *XMM-Newton* by Zane et al. (2005). The EPIC-PN count rate (background corrected) is ~ 1.6 count/s (in the 0.12-1.2 keV band), while the 0.2-2 keV unabsorbed flux is $\sim 5 \times 10^{-12}$ erg cm⁻²s⁻¹. The EPIC-PN spectrum is very soft and well fitted by an absorbed blackbody with $kT \sim 104$ eV and $N_H \sim 3.6 \times 10^{20}$ cm⁻². There is evidence for a spectral absorption feature at ~ 0.7 keV, and for a periodicity at 9.437 s (4σ confidence level) with a

¹ Mullard Space Science Laboratory, University College London Holmbury St Mary, Dorking, Surrey, RH5 6NT, UK

² Department of Physics, University of Padova, via Marzolo 8, I-35131 Padova, Italy

³ Università degli Studi dell’Insubria, Dipartimento di Fisica e Matematica, via Valleggio 11, 22100 Como, Italy

⁴ Max-Planck Institut für extraterrestrische Physik, Giessenbachstrasse, 85748 Garching, Germany

⁵ Observatoire Astronomique, 11, rue de l’Université, F-67000 Strasbourg, France

⁶ INAF-Astronomical Observatory of Padova, Vicolo dell’Osservatorio 5, I-35122 Padova, Italy

⁷ The detection of pulsed emission from two sources has been claimed at very low frequencies (Malofeev et al. 2005, 2006) but is, so far, unconfirmed.

pulsed fraction of $\sim 4\%$ in semiamplitude (Zane et al. 2005; Cropper et al. 2007).

The first optical follow-ups with the *NTT* and with the *VLT* revealed no optical counterpart within the *XMM-Newton* error circle, down to limiting magnitudes of $R \sim 22.8$ (Zampieri et al. 2001; Zane et al. 2005) and $V \sim 25.5$ (Mignani et al. 2007a), respectively. Additional optical (B, V, r' , i') and infrared (J, H and Ks) observations of RBS1774 performed with the Keck, *VLT*, Blanco and Magellan telescopes were recently reported by Rea et al. (2007), exploiting the subarcsec position obtained through a DDT *Chandra* observation. Again, no plausible optical and/or infrared counterpart for RBS1774 was detected down to $r' \sim 25.7$ and $J \sim 22.6$. Radio observations carried out with the Parkes 64m telescope at 2.9 GHz and 708 MHz were also reported by Rea et al. (2007). However, they did not show evidence for radio pulsations down to a luminosity of $L = 0.02$ mJy kpc^2 at 1.4 GHz. Very recently Kondratiev et al. (2008) placed more stringent upper limits on the radio luminosity of RBS1774, $L_{1.4\text{GHz}} \sim 0.005$ and ~ 7.6 mJy kpc^2 for pulsed and bursty emission respectively, which are the most stringent limits obtained to date from radio observations of XDINSs.

In this paper, we present the first detection of a candidate optical counterpart to RBS1774, obtained with the *VLT*. The observations and data analysis are described in § 2, while discussion and conclusions follow in § 3 and § 4, respectively.

2. THE NEW *VLT* OBSERVATIONS

2.1. Observations description

We performed deep optical imaging of the RBS1774 field with *FORS1* (FOcal Reducer Spectrograph), a multi-mode instrument for imaging and long-slit/multi-object spectroscopy mounted at the *VLT* Kueyen telescope (Paranal Observatory). The instrument has been recently upgraded with the installation of a new detector which is the mosaic of two $2\text{k} \times 4\text{k}$ E2V CCDs, optimized for the blue range. Due to vignetting, the effective sky coverage of the two CCD chips is smaller than the projected detector field of view, and larger for the upper chip (dubbed “Norma”). Observations were carried out in Service Mode on July 11th and 21st 2007. *FORS1* was set up in its default standard resolution mode, with a 2×2 binning, yielding a pixel size of $0''.25$. The telescope pointing was set in order to position our target on the “Norma” CCD chip, and, thanks to its large effective sky coverage (7×4 arcmin), to include a large number of reference stars for a precise image astrometry. The low gain, fast read-out mode was chosen. Sequences of 590 s exposures were obtained through the B Bessel filter ($\lambda = 429$ nm; $\Delta\lambda = 88$ nm), for a total integration time of 8850 and 2950 s in the first and second night, respectively. The observations were collected in dark time, with an average seeing of $\sim 0''.7$ and $\sim 0''.9$ and an airmass $\sim 1.17 - 1.37$ and ~ 1.18 on the first and second night, respectively.

2.2. Data reduction

The usual reduction steps (bias subtraction, flat-fielding) were applied to the data through the ESO

FORS1 data reduction pipeline⁸ using calibration frames acquired as part of the *FORS1* calibration plan. Then, single reduced images were aligned and coadded to filter out cosmic rays using the IRAF task *imcombine*. The photometric calibration was performed through the observation of standard stars from the fields PG 1323–086, PG 1633+099, SA 113–239 (Landolt 1992) at the beginning of the night. This yielded nominal extinction and color-corrected zero points of 28.16 ± 0.04 and 28.17 ± 0.04 for the first and the second night, respectively. The atmospheric extinction correction was applied using the extinction coefficients of the Paranal Observatory measured with the upgraded *FORS1* ($k_B = 0.255$ for the “Norma” chip). Since the zero point computed by the *FORS1* pipeline is in units of e^-/s , while the flux on the image is measured in ADU/s, we corrected the computed zero point by applying the detector electrons-to-ADU conversion factor ($\text{GAIN} = 0.45$). According to the Paranal Observatory sky monitor and weather report, sky conditions were photometric on the first night and at the beginning of the second night but they were then affected by the presence of thin, variable cirri. This means that the photometry of the second night is affected by a random, unknown uncertainty. We have tried to quantify this uncertainty by comparing the photometry of a number of reference field stars observed in the two nights. The star detection was performed using the *SExtractor* program and magnitudes were computed through customized aperture photometry (*SExtractor* parameter *MAG_AUTO*). In all sources detected at the flux level expected for our target ($B \geq 26$), we found an average offset of $\sim 0.1 \pm 0.5$ magnitudes between the photometry of the two nights. Such a large scatter for faint objects is due to the fact that their flux measurement is more sensitive on the varying atmospheric conditions than that of the bright ones. Thus, if data of the two nights are combined, this would result in only a modest increase of the S/N ratio at the expenses of a worse photometric accuracy for our target. We thus decided not to use the data taken on the second night.

2.3. Astrometry

The astrometry on the *FORS1* image was computed using as a reference the coordinates of stars selected from the *GSC-2* (version 3.2; Lasker et al. 2008). All stars from the *UCAC-2* (Zacharias et al. 2004) are saturated in our images. Approximately 90 *GSC-2* objects are identified in the *FORS1* “Norma” field of view. After filtering out extended objects, stellar-like objects that are saturated or too faint to be used as reliable astrometric calibrators, objects falling close to the chip edges, and outliers, we performed our astrometric calibration using 20 *GSC-2* reference stars, evenly distributed in the instrument field of view. Their pixel coordinates were measured by Gaussian fitting their intensity profiles with the GAIA (Graphical Astronomy and Image Analysis) tool⁹ while the fit to the celestial reference frame was performed using the Starlink package *ASTROM*¹⁰. This code is based on higher order polynomials, which account for unmodelled CCD distortions. The rms of the astro-

⁸ www.eso.org/observing/dfo/quality/FORS1/pipeline

⁹ star-www.dur.ac.uk/pdraper/gaia/gaia.html

¹⁰ star-www.rl.ac.uk/Software/software.htm

metric solution was determined as $\approx 0''.11$, per coordinate. Following Caraveo et al. (1998), we estimated the overall uncertainty of our astrometry by adding in quadrature the rms of the astrometric fit and the accuracy with which we can register our field on the *GSC-2* reference frame. This is estimated as $\sqrt{3} \times \sigma_{GSC} / \sqrt{N_s}$, where the $\sqrt{3}$ term accounts for the free parameters (x-scale, y-scale, and rotation angle) in the astrometric fit, σ_{GSC} is the mean (radial) error of the *GSC-2* coordinates ($0''.3$; Lasker et al. 2008) and N_s is the number of stars used for the astrometric calibration. The uncertainty on the reference stars centroids is well below 0.1 pixel and has been neglected. We also added in quadrature the radial uncertainty on the tie of the *GSC-2* to the ICRF ($0''.15$; Lasker et al. 2008). Thus, the overall radial accuracy of our astrometry is $0''.24$ (1σ).

2.4. Results

Fig. 1 shows a section of the co-added *FORS1* B-band image of the RBS1774 field. Fig. 1 (right) shows a zoom with the *Chandra* position of RBS1774 overlaid. The coordinates of RBS1774 were measured with high precision using *Chandra* HRC observations by Rea et al. (2007): $\alpha(J2000)=21^h 43^m 03.38^s$, $\delta(J2000)=+06^\circ 54' 17''.53$ with a nominal accuracy of $0''.6$ at the 90% confidence level (c.l.). The *Chandra* observation was recently reprocessed (December 2007) using updated calibration data products, and revised coordinates were obtained, $\alpha(J2000)=21^h 43^m 03.40^s$, $\delta(J2000)=+06^\circ 54' 17''.79$ (with the same nominal accuracy; Israel, private communication), which are consistent with the published ones. For comparison, in Fig.1 we show both the original and the revised error circles at the 90% and 99% c.l. The size of the error circles also accounts for the overall uncertainty of our astrometric calibration.

As is evident, a very faint object is detected about $0''.2$ from both the original and revised X-ray position. The object profile is point-like and consistent with the measured PSF, which, at the level of the *FORS1* spatial resolution, rules out the possibility of blending of fields object. We computed its magnitude through aperture photometry, by using a customized aperture and background region, following the same procedure described in the previous sections. The background was computed in an annular region centered on the target, in order to have the most reliable estimate close to the position of our source.

The measured value, corrected for the atmospheric extinction using the trended *FORS1* extinction coefficients, is $B=27.4 \pm 0.2$ (significant at $\sim 9\sigma$) where the quoted error (1σ c.l.) is purely statistical and does not include the much smaller errors on the zero point and on the atmospheric extinction correction. No other object is detected within or close to the *Chandra* position down to a 3σ limit of $B \sim 28.7$. As pointed out in the previous sections, the *FORS1* coordinates are tied to the ICRF within $0''.15$ so that we exclude a hypothetical shift with respect to the *Chandra* coordinates which are also tied to the ICRF¹¹. Thus, given its very good coincidence with the X-ray position, we regard this object as a viable candidate counterpart to RBS1774.

¹¹ <http://cxc.harvard.edu/cal/ASPECT/celmon/>

3. DISCUSSION

In this paper, we report the first detection of a likely optical counterpart for RBS1774. Standardly, optical identifications of isolated neutron stars are robustly confirmed either by the detection of optical pulsations or by the measurement of a significant proper motion. In absence of such information we can base the optical identification only on the positional coincidence between the coordinates of our candidate counterpart and those of RBS1774, as measured in the X-rays. In order to quantify the statistical significance, we estimated the chance coincidence probability that an unrelated field object might fall within the *Chandra* error circle. This can be computed as $1 - \exp(-\pi\mu r^2)$ (see, e.g., Severgnini et al. 2005), where μ is the measured object density in the *FORS1* “Norma” field of view and r is the registered radius of the *Chandra* error circle ($0''.65$, accounting for the uncertainty of the *FORS1* astrometry while the uncertainty due to the unknown RBS1774 proper motion is negligible given the small time span between the *Chandra* and *VLT* epochs). The measured density of stellar objects in the field with magnitude $27.2 \leq B \leq 27.7$, i.e. comparable to that of our candidate counterpart, is $\sim 0.0015/\text{sq arcsec}$. This yields an estimated chance coincidence probability $P \sim 2 \times 10^{-3}$ which shows that our association is robust.¹² Thus, we are confident that we have identified a very likely optical counterpart to RBS1774.

The flux of our candidate counterpart in the B band, after correcting for interstellar extinction, is $F_B = (2.55 \pm 0.47) \times 10^{-7}$ keV/cm²/s (the error is at 1σ c.l.). To compute this value, we used the column density derived from the best fit to the *XMM-Newton* spectrum ($N_H = 3.60 \times 10^{20}$ cm⁻², Cropper et al. 2007), with the A_V derived according to the relation of Predehl & Schmitt (1995).¹³ The interstellar extinction in the B-band has been computed using the extinction coefficients of Fitzpatrick (1999). When compared to the extrapolation in the B band of the blackbody which best-fits the *XMM-Newton* spectrum, $F_{B,x} = 7.36 \times 10^{-9}$ keV/cm²/s (Cropper et al. 2007), this gives an optical excess of 35 ± 20 (at 3σ c.l.), where all the uncertainties on the magnitude-to-flux conversion are negligible. The result is shown in Fig. 2, where the optical/IR upper limits of Rea et al. (2007) are also overplotted. The optical excess is larger than that typically observed in other XDINSs, and this may cast some doubts on the association of the newly detected source with RBS1774. On the other hand, if, as we suggest, the association is real, it can be used to infer physical constraints on the mechanism that is responsible for the optical emission.

The first scenario we consider is one in which the optical emission originates from a cooler fraction of the neutron star surface, which emits as a blackbody at temperature T_o (Braje & Romani 2002; Pons et al. 2002;

¹² If we compute the chance probability by considering all objects brighter than $B=27.7$, we get a very similar result, $P = 2.3 \times 10^{-3}$.

¹³ The Predehl & Schmitt (1995) relation is affected by uncertainties for close objects, due to the problems of modelling the ISM at small distance from the Sun where microstructures weight more. We checked that, when using the relations of Bohlin et al. (1978), as in Rea et al. (2007), and of Paresce (1984) extinction corrections are consistent within 0.04 magnitudes, well below the pure statistical error on the source count rate.

Kaplan et al. 2003b; Trümper et al. 2004)¹⁴. In this case, the ratio between the optical and X-ray fluxes scales as $\approx r_o^2 T_o / r_x^2 T_x \equiv f$, where r_o is the radial size of the cold region (which of course can not exceed the maximum value of the neutron star radius), r_x and T_x are the blackbody radius and temperature as inferred from the X-ray spectrum, $T_x = 104$ eV, $r_x = 2(d/300 \text{ pc})$ km (Cropper et al. 2007). By making an assumption on r_o we can obtain the lower limit on T_o that corresponds to values of f between the central value and the 3σ lower limit ($15 \leq f \leq 35$). Furthermore, since no contribution from such a cold component is observed in the 0.1-1 keV *XMM-Newton* spectrum, it must be $R \ll 1$, where

$$R = \left(\frac{r_o}{r_x}\right)^2 \left(\frac{T_o}{T_x}\right)^4 \frac{\int_{0.1/T_o}^{1/T_o} t^3 / (\exp(t) - 1) dt}{\int_{0.1/T_x}^{1/T_x} t^3 / (\exp(t) - 1) dt}. \quad (1)$$

We repeated this calculation by varying the distance between 200 and 500 pc¹⁵ and for $r_o = 20, 15$ or 10 km. Results show that this scenario is only barely compatible with our data and requires very small distances: $d \sim 300 - 400$ pc are only allowed within 3σ and for neutron star radii as large as $r_o = 20$ km, while if $r_o = 15$ km the only allowed combinations require $f = 15 - 22$ and $d \sim 200 - 250$ pc. On the other hand, the lower the distance the smaller is the size of the X-ray emitting region and the more difficult is to explain the small pulsed fraction observed in the X-rays (which is $\sim 4\%$ in semi-amplitude). As we tested by assuming simple polar cap modelling and blackbody emission, if $d = 300$ pc the allowed parameter space is already confined to a very small region where the inclination angles of the line of sight and of the magnetic dipole axis with respect to the star spin axis are both $\lesssim 20^\circ$. If $d = 200$ pc, the allowed region is even smaller and the only possible configurations require the star to be either a perfectly aligned rotator or viewed almost along its spin axis.

As discussed by Motch et al. (2003), Zane et al. (2004) and Ho et al. (2007), spectral models consisting of bare neutron stars surrounded by thin atmospheres may predict very different amount of optical excess. However, such models are affected by our poor knowledge of the properties of the condensate surface, and whether they can produce optical excesses as large as that measured here is still an open issue.

An alternative interpretation is that the optical emission is non thermal, probably of magnetospheric origin (Pacini & Salvati 1983). As it can be seen from Fig. 2, a power law spectral component $E^{-\alpha}$ matching the B-flux and with index $\alpha \sim 0 - 1.4$ is not in contradiction with the upper limits measured at longer wavelengths and, at the same time, is not expected to contribute significantly to the X-ray band. These constraints on the optical spectral index are compatible with the values determined from the optical spectra of rotation-powered neutron stars, which are all in the range 0–0.8 (see, e.g., Mignani et al. 2007b). In this respect, we note that for the XDINSs for which the spin down luminosity is measured (Cropper et al. 2004; Kaplan & van Kerkwijk

2005a,b; Van Kerkwijk & Kaplan 2008) it is $\dot{E} \sim 5 \times 10^{30}$ erg/s. If the case of RBS1774 is analogous, and if we take $L_{opt}/\dot{E} \approx 10^{-6}$ for the optical emission efficiency (as measured in old rotation-powered neutron stars by Mignani et al. 2004), this yields an optical luminosity of $\sim 5 \times 10^{24}$ erg/s. In order to reproduce the observed flux of our candidate counterpart, after accounting for the assumed interstellar extinction, RBS1774 should be at an unrealistically small distance of ~ 25 pc. Thus, for the assumed value of \dot{E} , a purely rotation-powered optical emission is only compatible with a scenario in which our source is at least a two orders of magnitude more efficient optical emitter (see below). Similar conclusions can be reached if we consider the case in which the observed optical emission of RBS1774 is due to a composite mechanism consisting of both thermal emission from the neutron star surface and a rotation-powered magnetospheric emission (as in the middle-aged neutron stars PSR B0656+14 and Geminga, e.g. Kargaltsev & Pavlov 2007).

A further, intriguing possibility is that the optical emission is non-thermal and powered by a mechanism different from rotation. Interestingly, at least in the IR domain, hints have been found for an increase of the low-energy emission efficiency with the dipole magnetic field strength (Mignani et al. 2007c). Indeed, in magnetars the efficiency is at least two orders of magnitude larger than in rotation-powered neutron stars and the spectra show a typical (and unexplained) flattening toward the infrared (Israel et al. 2003). It is interesting to note the magnetic field strength of RBS1774 as inferred from the absorption feature in the X-ray spectrum is the highest among all XDINSs ($B \approx 10^{14}$ G), larger than the QED critical limit and comparable with that of magnetars. The optical emission of RBS1774 could thus be powered by a magnetar-like process. If the spectrum of RBS1774 shows a similar magnetar-like turn over, then the flattening is appearing blueward of the IR band.

4. CONCLUSIONS

We report here the deepest optical observations so far of the RBS1774 field, performed with the upgraded *FORSl* instrument at the *VLT* Kueyen telescope. Based on the positional coincidence, we have identified a likely candidate counterpart. RBS1774 would then be the fifth XDINS detected in the optical band, the second by the *VLT*. For the most reasonable distance range to the X-ray source, the measured brightness of the candidate counterpart ($B \sim 27.4$) is barely compatible with purely thermal emission from the neutron star surface, while, assuming a value of \dot{E} similar to that of other XDINSs, rotation-powered emission from the magnetosphere (eventually in combination with a thermal component) requires RBS1774 to have a very large optical efficiency (~ 3 order of magnitudes larger than the Crab for $d = 400$ pc). If the optical emission is powered by a different process, the likely high magnetic field of RBS1774 tantalizingly suggests magnetar-like magnetospheric emission as a viable option. New multi-band observations, especially in the near-UV and in the near-IR, are required to characterize the counterpart spectrum and to assess the contribution of possibly different spectral components. At the same time, high resolution optical astrometry of the candidate counterpart with the

¹⁴ Note, however, that when applied to other XDINSs this scenario often requires large neutron star radii.

¹⁵ We do not use the distance determination by Posselt et al. (2007), since their model is currently under revision for the case of RBS1774 (Posselt, private communication).

refurbished *HST* could yield the first direct estimate of the RBS1774 parallax and distance, crucial to build the neutron star surface thermal map, and to provide confirmation of the optical counterpart through proper motion measurements.

SZ acknowledges support from a STFC (ex-PPARC)

AF. RM acknowledges STFC for support through a Rolling Grant. RT acknowledges financial support from ASI-INAF through grant AAE TH-058. LZ acknowledges financial support from ASI-INAF through grant I/023/05/0.

REFERENCES

- Bohlin, R.C., Savage, B. D., Drake, J. F. 1978, *ApJ*, 224, 132
 Braje, T.M., Romani, R.W. 2002, *ApJ*, 580, 1043
 Caraveo, P.A., Lattanzi, M.G., Massone, G., et al. 1998, *A&A*, 329, L1
 Cropper, M. et al. 2004, *MNRAS*, 351, 1099
 Cropper, M. et al. 2007, *Ap&SS*, 308, 161
 Fitzpatrick, E.L., 1999, *PASP*, 111, 63
 Haberl, F. 2007, *Ap&SS*, 308, 181
 Heyl, J.S. & Kulkarni, S.R. 1998, *ApJ*, 506, L61
 Ho, W.C.G., et al. 2007, *MNRAS*, 375, 821
 Israel, G.L. et al. 2003, *ApJ*, 589, L93
 Kargaltsev, O.Y., Pavlov, G.G. 2007, *Ap&SS*, 308, 287
 Kaplan, D.L., Kulkarni, S., Van Kerkwijk, M.H. 2003a, *ApJ*, 588, L33
 Kaplan, D.L., et al. 2003b, *ApJ*, 590, 1008
 Kaplan, D.L., van Kerkwijk, M.H. 2005a, *ApJ*, 628, L45
 Kaplan, D.L., van Kerkwijk, M.H. 2005b, *ApJ*, 635, L65
 Kaplan, D.L. 2008, proceedings of "40 Years of Pulsars: Millisecond Pulsars, Magnetars, and More", August 12-17, 2007, McGill University, Montreal, Canada, AIP, 983, 331
 Kondratiev, V.I. et al. 2008, submitted to *ApJ*
 Landolt, A.U. 1992, *AJ*, 103, 340
 Lasker, B.M. et al. 2008, submitted to *AJ*
 Malofeev, V.M. et al. 2005, *Astr. Rep.*, 49, 242
 Malofeev, V.M. et al. 2006, *ATel* #798;
 McLaughlin, M.A. et al. 2006, *Nature*, 439, 817
 McLaughlin, M.A. et al. 2007, *ApJ*, 670, 1307
 Mereghetti, S. 2008, arXiv:0804.0250, submitted to *Astronomy and Astrophysics Review*
 Mignani, R.P., De Luca, A., Caraveo, P.A. 2004, in Proc. of "Young Neutron Stars and Their Environments", IAU Symp. 218, eds. F. Camilo and B. Gaensler, ASP Conf. Proc., p. 391
 Mignani, R.P. et al. 2007a, *Ap&SS*, 308, 203
 Mignani, R.P., Zharikov, S., Caraveo, P.A. 2007b, *A&A*, 473, 891
 Mignani, R.P. et al. 2007c, *A&A*, 471, 265
 Motch, C., Zavlin, V.E., Haberl, F. 2003, *A&A*, 408, 323
 Motch, C., et al. 2005, *A&A*, 429, 257
 Pacini, F., Salvati, M. 1983, *ApJ*, 274, 369
 Paresce, F. 1984, *AJ*, 89, 1022
 Pons, J.A., et al. 2002, *ApJ*, 564, 981
 Popov, S.B., Turolla, R., Possenti, A. 2006, *MNRAS*, 369, L23
 Posselt, B. et al. 2007, *Ap&SS*, 308, 171
 Predehl, P. & Schmitt, J.H.M.M. 1995, *A&A* 293, 889
 Rea, N. et al. 2007, *MNRAS*, 379, 1484
 Severgnini, P. Della Ceca, R., Braito, V., et al., 2005, *A&A*, 431, 87
 Skrutskie, M. F., et al. 2006, *AJ*, 131, 1163
 Trümper, J.E., Burwitz, V., Haberl, F., Zavlin, V.E. 2004, *Nuclear Physics B Proceedings Supplements*, 132, p. 560-565.
 van Kerkwijk, M.H., Kaplan, D.L. 2007, *Ap&SS*, 308, 191
 van Kerkwijk, M.H., Kaplan, D.L. 2008, *ApJ*, 673, L163
 Zacharias, N., et al. 2004, *AJ*, 127, 3043
 Zampieri L., et al. 2001, *A&A*, 378, L5
 Zane, S., Turolla, R., Drake, J.J. 2004, *AdSpR*, 33, pp. 531-536.
 Zane, S., et al., 2005, *ApJ*, 627, 397
 Zane, S., et al. 2006, *A&A*, 570, 619

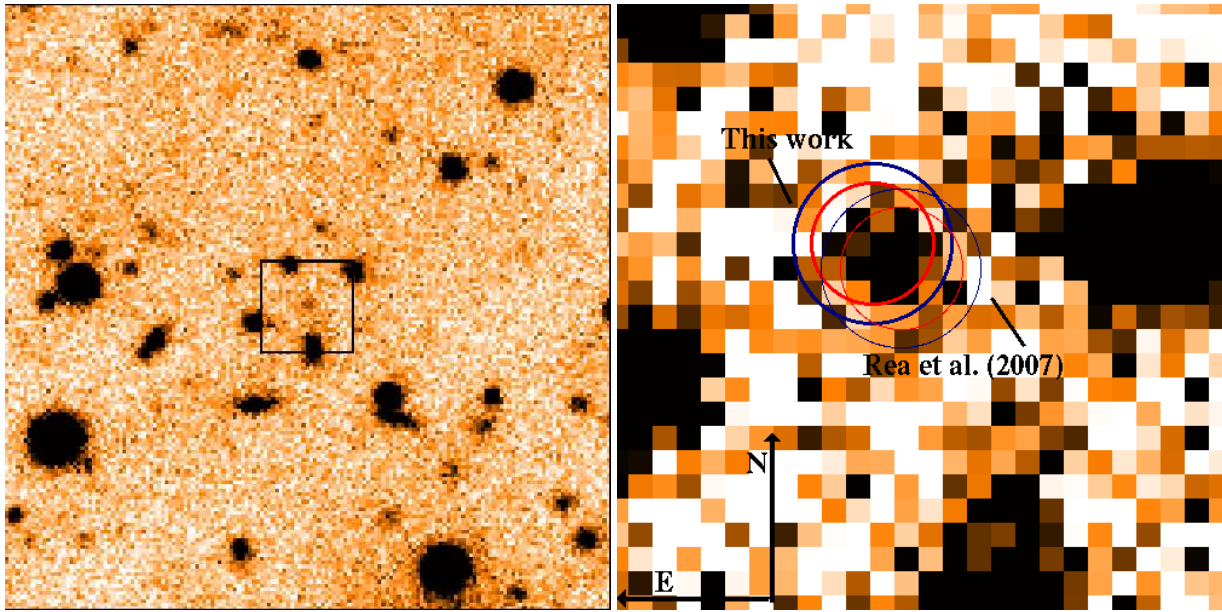


FIG. 1.— *Left.* B -band image ($40'' \times 40''$) of the RBS1774 field obtained with *FORS1* at the *VLT* Kueyen telescope. The square corresponds to the $6'' \times 6''$ zoom shown in the right-hand panel. The intensity scale has been re-adjusted for an easier view of the brighter objects in the field. *Right.* $6'' \times 6''$ zoom of the same field. The circles correspond to the original (Rea et al. 2007) and revised (this work, §2.4) *Chandra* position of RBS1774, and are drawn at the 90% (red) and 99% (blue) confidence level. Their size ($0''.65$ and $0''.85$, respectively) also accounts for the uncertainty of the astrometric calibration of the *FORS1* image. The object detected at the centre of the error circles ($B = 27.4 \pm 0.2$) is our candidate counterpart to RBS1774.

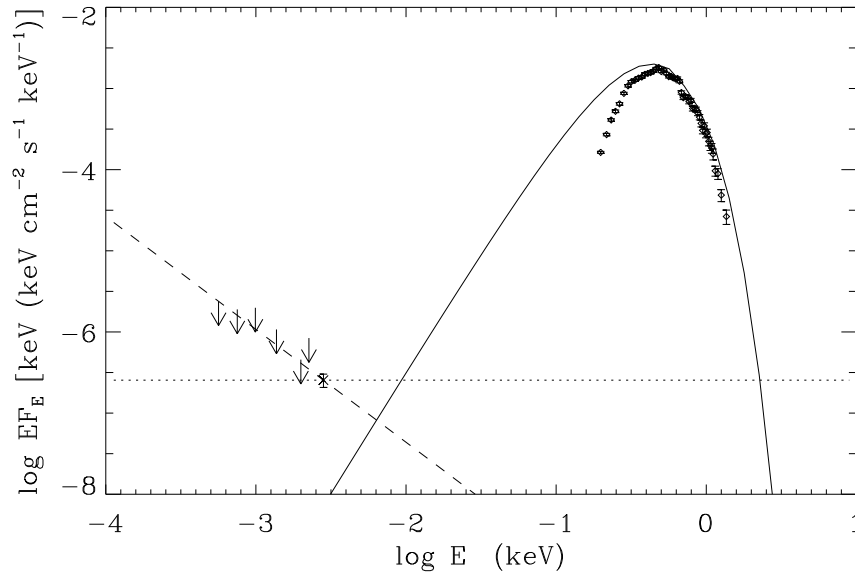


FIG. 2.— Multi-band spectrum of RBS1774. Diamonds represent the *XMM-Newton* spectrum (Zane et al. 2005). The solid line shows the unabsorbed blackbody that best fits the X-ray data, while arrows represent the 5σ upper limits reported by Rea et al. (2007). The new *VLT* measurement is shown as a cross. Dotted and dashed lines represent two powerlaw components matching the B -flux and with slope $\alpha = 0, 1.4$, respectively. Figure re-adapted from Rea et al. (2007).